ELSEVIER

Polymer 42 (2001) 2121–2135

polymer

www.elsevier.nl/locate/polymer

A study of the phase behaviour of polyethylene blends using micro-Raman imaging

R.L. Morgan[a,1], M.J. Hill[a,*], P.J. Barham[a], A. van der Pol[b], B.J. Kip[b], R. Ottjes[b], J. van Ruiten[b]

[a]*H.H.Wills Physics Laboratory, University of Bristol, Tyndall Avenue, Bristol BS8 1TL, UK*
[b]*DSM Research, P.O. Box 18, 6160 MD Geleen, The Netherlands*

Received 24 September 1999; received in revised form 6 April 2000; accepted 14 June 2000

Abstract

The origin of morphological phase structures in blends of a linear deuterated polyethylene and a hydrogenous branched polyethylene has been investigated using Raman imaging. Blends were crystallized to produce samples with large domains that are rich in linear material surrounded by a matrix that is rich in branched polymer. The samples were then remelted for a range of holding times and quenched to examine the remixing of the separated domains in the melt. The micro-Raman images show that the samples remixed to a homogeneous distribution by branch content within the expected time scale, as estimated from the diffusion constants. However, micro-Raman imaging was also used to detect crystallinity variations and it reveals a biphasic structure in quenched blends that display a morphological phase structure when examined in the transmission electron microscope. Raman images of the same samples are uniform when constructed by branch content. Possible causes for this phenomenon are briefly discussed.

Keywords: Polyethylene blends; Raman imaging; Phase separation

1. Introduction

The determination of the miscibility in the melt of different polyethylenes has attracted considerable interest in recent years. The interest is generated by the commercial practice of blending the materials to achieve desirable properties and the need to understand heterogeneous materials containing molecules with a wide range of molecular structures. There is widespread agreement that blends composed of linear polyethylenes with branched polyethylenes exhibit lower critical phase behaviour when the branch content is above a critical level [1]. The degree of miscibility in blends containing only lightly branched polyethylenes has, however, generated some controversy. In this paper we address the issue of miscibility in these latter systems using micro-Raman imaging.

Studies of the morphologies of blends of homopolymers with their branched copolymers have been proceeding at the University of Bristol for the past decade [2–19]. The work, which arose from unexplained morphological observations, has largely, but not exclusively, dealt with linear polyethylenes (LPE) blended with lightly branched polyethylenes (BPE). Biphasic morphologies were observed in some blends, quenched from certain temperatures. These observations led to the conclusion that under certain circumstances the melts could phase separate. However, the chemical similarity of these materials hinders the direct study of the melt. Consequently, indirect methods have been developed, which involve the study of the solid state structure after quenching from the melt. The cooling rates employed are believed to be sufficiently fast to 'freeze in' the melt structure.

The principle analytical techniques used are differential scanning calorimetry (DSC) and transmission electron microscopy (TEM). Two types of crystal, separated on a scale of microns, are detected on quenching blends of some compositions from some temperatures. However, only one crystal type is detected on quenching the same samples from higher temperatures, and on quenching blends of other compositions from all temperatures. TEM observations show the two crystal types to be separated on a scale of microns within a morphological phase structure. We have shown that the phase structure ripens with residence time in the pre-quenched melt, in accordance with classical Ostwald ripening theory [14]. The simplest explanation for these results would seem to be that liquid–liquid phase separation occurs between blend components.

For many polyethylene blend systems, morphology maps,

* Corresponding author.
[1] Current address: Smith and Nephew Group Research Centre, York Science Park, Heslington, York YO10 5DF, UK.

0032-3861/01/$ - see front matter
PII: S0032-3861(00)00449-3

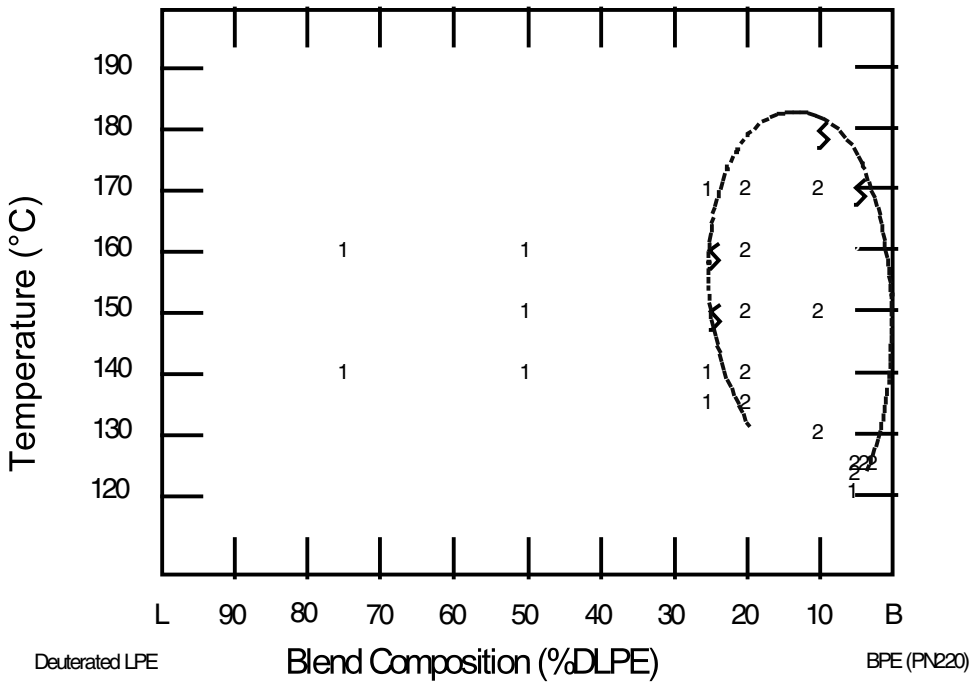

Fig. 1. Morphology map for the DLPE/BPE blend system studied in the present paper. This map was deduced from TEM studies of quenched blends. Sample points marked 1 indicated a single morphology and those marked 2 a biphasic morphology.

which, on the above arguments, would be interpreted as 'phase diagrams', have been produced using indirect techniques. A common characteristic of the morphology maps of binary blends of LPEs with lightly BPEs is that the region of liquid–liquid phase separation is in the form of a closed loop, situated at low LPE content. An example of such a morphology map (which has, in the past, been interpreted as a phase diagram) is shown in Fig. 1. If such a map is interpreted as a phase diagram, then it can be used to find the compositions of the two phases at any particular temperature. For instance, for a temperature of 150°C and an overall composition of 10% LPE, Fig. 1 indicates that one phase should contain a very small amount of LPE, while the other phase should contain about 25% of LPE. Neither of the components (DLPE or BPE) in this diagram are pure single component systems themselves; both contain a range of molecular weights and the BPE contains a range of differently branched molecules. Accordingly, it would never be correct to interpret our morphology maps as phase diagrams, but they could still be considered as cloud point diagrams. In such a case, there would be much less certainty concerning the expected compositions of the separated phases; but we would still expect that a 10% blend quenched from 150°C would contain two phases with distinctly different compositions.

The melt phase behaviour of LPE/BPE systems has also been studied by other research groups, some of whom have questioned the interpretation of the indirect, Bristol evidence. Alamo et al. [20] investigated blends of deuterated linear polyethylene (DLPE) with a low density polyethylene (LDPE), directly in the melt, using small angle neutron scattering (SANS). Phase separation, on a scale of up to 100 nm, was detected by SANS, and a thermodynamic interaction parameter was calculated for the components. However, phase separation has also been detected by SANS in blends of DLPE with hydrogenous LPE [21] and an interaction parameter of similar magnitude was calculated. Consequently, the authors of Ref. [20] considered the separation detected in the DLPE/LDPE system to be an isotope effect. After allowance for the effect of deuterium on phase behaviour, Alamo et al. concluded that LPEs and lightly branched polyethylenes are fully miscible in the melt. Schipp et al. have also studied the melts of DLPE/LDPE blends [15] and noted that micron scale separation would not be detected by existing SANS equipment. (Note that Schipp et al worked with blends of the very same polymers as have been used in the present work so their results are particularly relevant to these studies.) Alamo et al. [20] proposed that the segregation of the components in the solid state, reported by Bristol workers, was due to a crystallization mechanism rather than incompatibility in the liquid state. However, it has been demonstrated that when segregation through crystallization does occur during cooling, this segregation occurs on a significantly smaller scale (50–100 nm) than that of the double morphologies observed in quenched blends (1–2 μm) [22].

In an earlier paper [23] we reported the use of micro-Raman imaging to gain compositional information from polyethylene blends and we compared the images with morphologies. In order to distinguish the spectra of the two blend components, blends of a deuterated linear polyethylene and a hydrogenous, branched polyethylene were

Table 1
Characteristics of polymers

Material	M_w (g/mol)	M_w/M_n	Branch content (branches per 1000 carbon atoms)
DLPE	2×10^5	2	0
BPE	2×10^5	8	16 short, 10 long

used. Both isothermally crystallized and rapidly quenched blends were studied by Raman imaging, and the results were compared with those from TEM. The isothermally crystallized blends were prepared at very low undercooling, to generate large compositional differences on a large spatial scale. Both the compositional variations, between 0 and 40% LPE, and the compositional phase structures that we detected in isothermally crystallized blends agreed closely with the morphological phase structures detected by TEM. Compositional differences were not, however, detected by Raman imaging in the rapidly quenched blends studied. The morphological phase structures in such blends are on a scale of 1–2 μm, which is close to the limit of spatial resolution attainable by Raman imaging. On the basis of some simple modelling work, the maximum compositional difference which could be associated with the morphological phase structure, but which could remain undetected by Raman imaging, was calculated to be only 3%. These results raise the issue of whether such small variations in composition can, by themselves, generate the observed morphological phase structures.

In this paper we use Raman imaging to investigate the origin of the morphological phase structures and report two series of experiments. The first series involves studying the stability in the melt of the large-scale phase structures formed during isothermal crystallization. The reasoning behind this choice of experiment is that if the morphology maps should be interpreted as "phase diagrams" then the scale of the phase structure formed on remelting should not decrease from that present in the isothermally crystallized samples. The second experiment involves the measurement of crystallinity by Raman spectroscopy and the mapping of crystallinity variations for comparison with morphology.

2. Experimental

2.1. Preparation of the samples

The materials studied were blends of a deuterated linear polyethylene, obtained from Merck, Sharpe and Dohme, and a low density polyethylene, PN220, obtained from BP Chemicals. The characteristics of these polymers are shown in Table 1. The blends were made in a 0.4% solution with xylene and were co-precipitated using acetone as the non-solvent. This solution blending method has been discussed elsewhere in detail [2].

Samples were prepared in the form of bulk specimens at least 0.5 mm thick. Some samples were prepared on a Kofler hot-bench, between glass cover slips, and were subsequently quenched rapidly by flicking into acetone at its freezing point. Visual observation suggests that crystallization occurs in less than a second using this method. Other samples were prepared in an oil bath. Samples to be crystallized isothermally were held initially in the melt at a temperature of 150°C, in a separate oil bath, and then transferred rapidly to an oil bath at the chosen crystallization temperature. Crystallization temperatures were selected to be sufficiently low for the DLPE to crystallize, but not low enough for the BPE to crystallize to a significant extent in the time allowed. After holding at the crystallization temperature, for a time determined to be sufficient for completion of the DLPE crystallization, the samples were quenched by transfer into acetone at its freezing point. Samples which required holding in the melt for long times were sealed in evacuated glass tubes to prevent oxidation. The blend material was held within the tubes between small sections of cover slips. A polytetrafluroethylene, PTFE, spray was used to coat the glass, to aid sample removal. The tubes were fully immersed in oil and, after holding for a predetermined time, were quenched into acetone at its freezing point.

Samples for Raman imaging were microtomed to produce sections with a thickness of 2–3μm. The sections were mounted on quartz cover slips with tape. Fluorescence from quartz was observed to be significantly lower than from borosilicate glass.

2.2. Experiments to determine the stability of phase separated domains

We performed a series of experiments to determine the stability of phase separated domains using samples that had previously been well separated by slow, isothermal, crystallization. The isothermally crystallized blends were raised in temperature to a position within the double morphology loop of the morphology map shown in Fig. 1, and the compositional phase structures maintained as a function of time were monitored by Raman imaging. The following procedure was adopted for the phase stability measurements: blend material was crystallized isothermally at 118°C, quenched to below room temperature and then studied by Raman imaging. Samples from the isothermally crystallized material were melted and held at 150°C for different lengths of time. Each sample was quenched rapidly from 150°C and was subsequently studied by Raman imaging and TEM at room temperature. The procedure allows the remixing, phase separation or ripening behaviour of the initial, large-scale phase structures to be followed as a function of time by Raman imaging. Additionally, the morphological phase structures detected at each stage of the cycle can be compared with the compositional

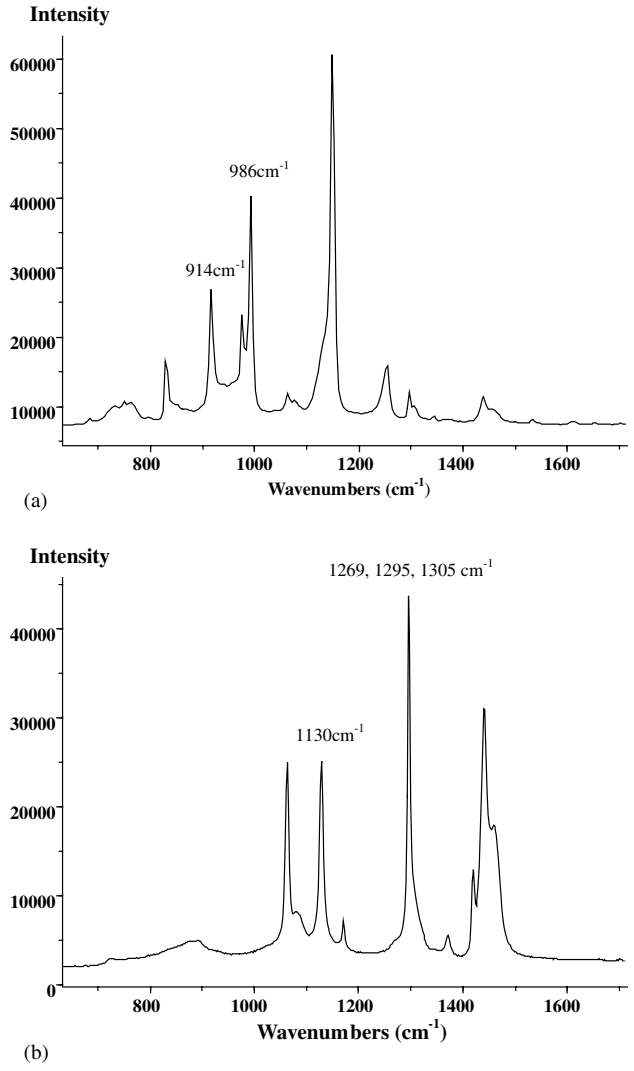

Fig. 2. (a) Raman spectrum of the deuterated linear polyethylene. The bands used for crystallinity measurements are indicated. (b) Raman spectrum of the hydrogenous branched polyethylene. The bands used for crystallinity measurements are indicated.

variations. Crystallinity maps were also constructed from a Raman imaging data set for samples held in the melt for more than 48 h.

2.3. Raman imaging

All Raman measurements were recorded with a Dilor Labram confocal Raman imaging system at DSM Research, Geleen. In this system a 25 mW Helium–Neon laser (Melles-Griot, wavelength 632.817 nm) or a 2 W Ar^+ ion laser (Spectra Physics 2000, wavelength 514.532 nm) is interfaced with an Olympus BX40 microscope. The microscope objective, used during imaging, had a magnification of 100× and a numerical aperture of 0.90. The confocal pinhole was of variable width. The details of confocal Raman imaging can be found elsewhere [24,25]. The spectrometer grating had 1800 lines/mm. The laser power at the sample was measured to be 4 mW (633 nm) or 25 mW (515 nm). A quarter wavelength plate was inserted into the laser beam to obtain circularly polarized light. The Raman scatter was collected on a peltier cooled, two-dimensional Spectrum One CCD camera (Jobin Yvon). The CCD contained 2000 by 800 detector elements, and the long axis of the CCD was used to collect spectral information. The sample was mounted on an XY-scanning stage, controlled by a stepper motor. Dilor Labspec 2.0 software was used to operate the imaging system, record the spectra and process the data. Raman images were recorded across two spatial dimensions by static point illumination combined with two dimensional sample movement.

The following procedure was adopted in recording spectra. The sample was inspected under the microscope, using white light, and a suitable region was chosen which appeared flat and showed no orientation effects. Raman spectra were recorded continuously, over short times, and the signal was optimized by positioning the focal object plane within the sample section to obtain a balance between the Raman signal and the weak Raman and fluorescence background of the quartz plate. The imaging area was selected by recording individual spectra from a series of points, in order to detect compositional variations. The variation in strength of the Raman scatter, over the chosen imaging area, was checked to ensure that the sample was flat and of even thickness. The imaging area, the number of spectra, the pinhole size and the spectral collection time were selected on the basis of the expected scale of features within the sample. For samples containing features on a scale of microns, the instrument was operated at maximum spatial resolution, with a pinhole width of 75 μm and with point to point distances of 0.5 or 0.75 μm. For samples containing features on a scale of over 5 μm a larger pinhole width was used, to allow shorter spectral collection times. It should be noted that since the samples were sections, with a thickness of 2–3 μm, the vertical spatial resolution is essentially limited by the sample thickness when the pinhole width is above approximately 150 μm.

Compositional images of the DLPE/BPE blends were based on the areas under CD_2 and CH_2 stretching Raman bands. The compositions were determined from the ratio of the areas of the two bands, after subtraction of a baseline. Calibration measurements were performed on homogeneous blends of a range of compositions, to allow conversion between the band area ratio and composition. Typically, 100 spectra from different points, recorded with a 10× objective, were averaged for each calibration sample. In blends containing regions of relatively high DLPE content (>30%) the CD_2 stretching band at 2100 cm^{-1} and the CH_2 stretching band at 2900 cm^{-1}, which are the strongest bands in the two spectra, were recorded. In blends where the DLPE content was low, for example 4% blends, the images were based on the CD_2 stretching band at 2100 cm^{-1} and the low intensity CH_2 stretching band at 2720 cm^{-1}; these are of similar intensity in such blends. After collection, the spectra

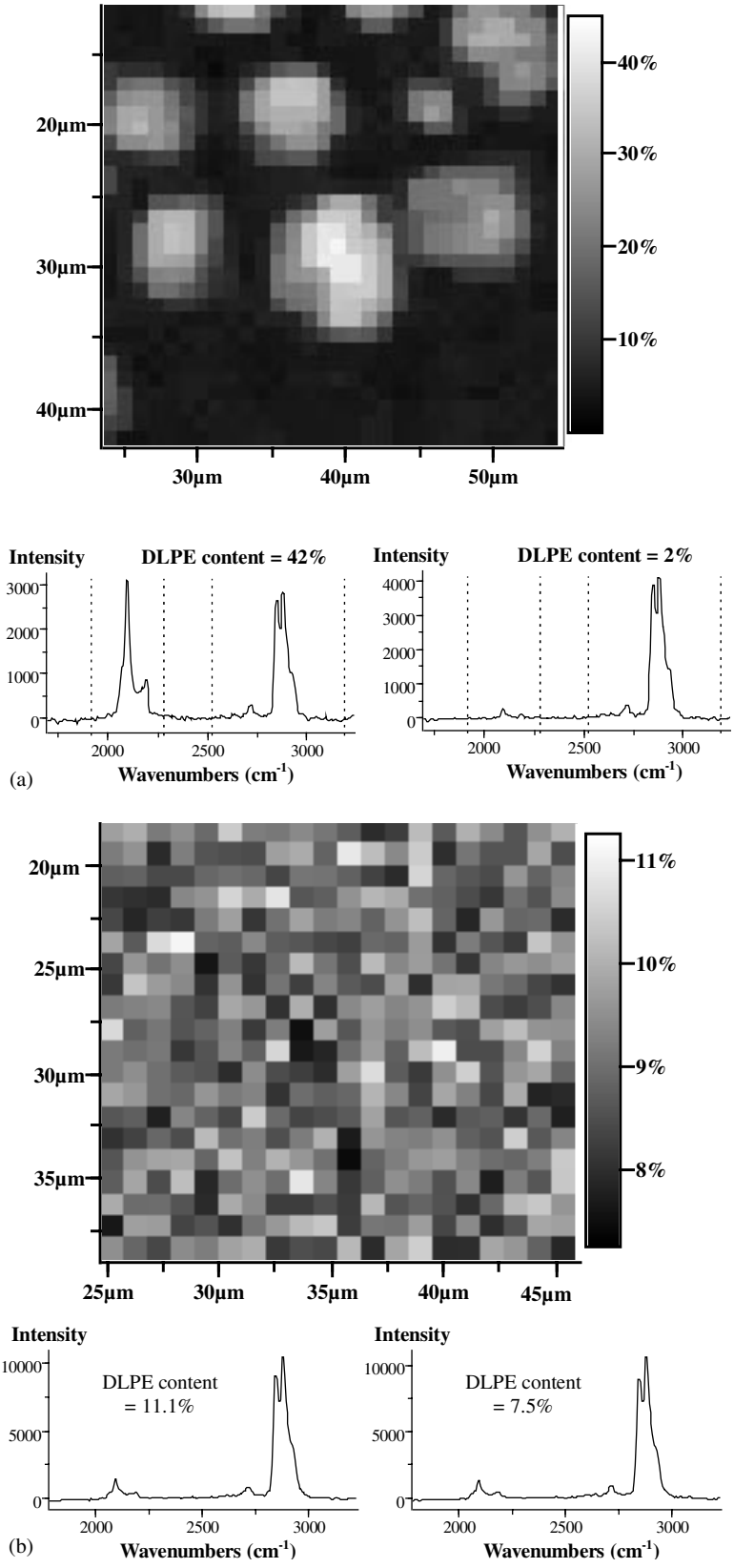

Fig. 3. Raman images of 10% blends, based on the ratio of the bands at 2100 and 2900 cm^{-1}. The pixel size is 1×1 μm^2. The figures also include spectra corresponding to the pixels for which maximum and minimum DLPE content were recorded. (a) Crystallized isothermally at 118°C. (b) crystallized isothermally at 118°C, remelted at 150°C, held for 48 h and then quenched.

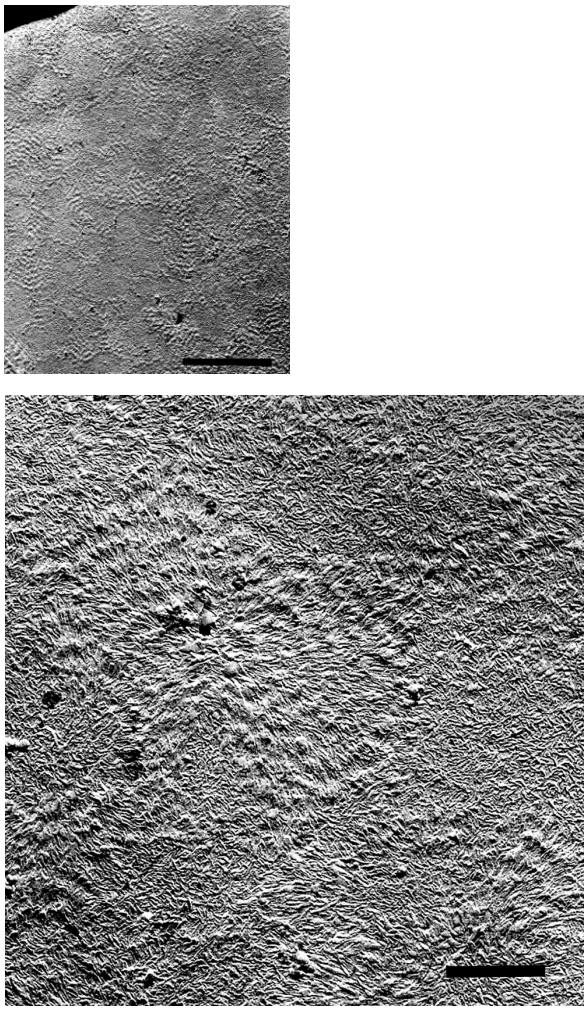

Fig. 4. Transmission electron micrograph of a replica of a 10% blend, after isothermal crystallization at 118°C and remelting at 150°C, where it was held for 48 h before quenching. There are micron sized regions of thicker crystals (with a banded appearance) and thinner crystals; the regions of both types can be seen in (a), at the same magnification as Fig. 3b (the scale bar in (a) represents 5 μm). (b) shows further detail, revealed in a higher magnification electron micrograph taken from a different part of the same sample. There is a region containing thicker crystals, arranged as a banded spherulite-like structure, just above and left of centre. The scale bar represents 1 μm.

were filtered to remove noise spikes. Crystallinity measurements were based on the concentration of all trans sequences. The amount of all trans sequences in the BPE is related to the integrated area of the band at 1130 cm^{-1}, normalized by the integrated area of the cluster of bands at 1269, 1295 and 1305 cm^{-1} [26,27]. The crystallinity (deduced from the amount of all trans sequences) of the deuterated polyethylene is related to the integrated area of the band at 986 cm^{-1}, normalized by the integrated area of the band at 914 cm^{-1} [28]. We have chosen not to calculate actual crystallinities, because of overlap between the spectra of the two blend components, but simply to quote band ratios. Fig. 2 shows the fingerprint region of the Raman spectra of both the DLPE and BPE, on which the positions and assignments of the bands used in the crystallinity calculations are indicated.

2.4. Transmission electron microscopy

Surface replicas were produced from samples etched using the Bristol modification [29] of the permanganic etching technique [30,31]. The replicas were studied in a Philips 400T TEM operating at 100 KeV.

3. Results and discussion

3.1. Phase stability experiments

Isothermally crystallized 10 and 4% blends were studied after melting and holding at 150°C. The isothermally crystallized samples contain large compositional variations (0–40% LPE), distributed over a scale of tens of microns. It is unlikely that these compositional phase structures will be stable at 150°C. If the morphology map, shown in Fig. 1, is interpreted as a phase diagram, then the equilibrated melts of both blends should be separated into two phases, one phase with almost no DLPE and one phase with about 25% of DLPE, at 150°C. Alternatively, the morphology map may not describe phase behaviour, in which case the two blend components could be fully miscible at 150°C. Either way, one would expect some changes in the melt composition on remelting the isothermally crystallized blend at 150°C; the details of this diffusion process should yield further information about the nature of the melts of the blends. Isothermally crystallized samples were held at 150°C for predetermined times and were then quenched to preserve their phase structures. Raman imaging and TEM were used to study the quenched samples.

Fig. 3a shows a compositional Raman image of a 10% blend crystallized isothermally at 118°C. Fig. 3b shows the image of the same sample after remelting and holding for 48 h at 150°C. Very little compositional variation can be seen in the Raman image of the remelted sample and we suggest that this small variation is simply the result of spectral baseline variations. An estimate of the error in the integration method was obtained by integrating between different limits and resulted in an absolute variation of ±1%. The measured variation in composition across the image is, therefore, close to the limit of estimated error. The average composition for the whole image was calculated to be 9.1%, in good agreement with the overall blend composition. It would appear, therefore, that the compositional phase structure in the isothermally

Fig. 5. Raman images of 4% blends, all of which were crystallized isothermally at 118°C. Some of the samples (b–e) were remelted and held at 150°C for the times shown below, before quenching to room temperature. The images are based on the ratio of the areas under the bands at 2100 and 2720 cm^{-1}. Note that imaged areas vary and that the images have been scaled accordingly. (a) Not remelted; (b) 2 min; (c) 20 min; (d) 2 h; (e) 5 h.

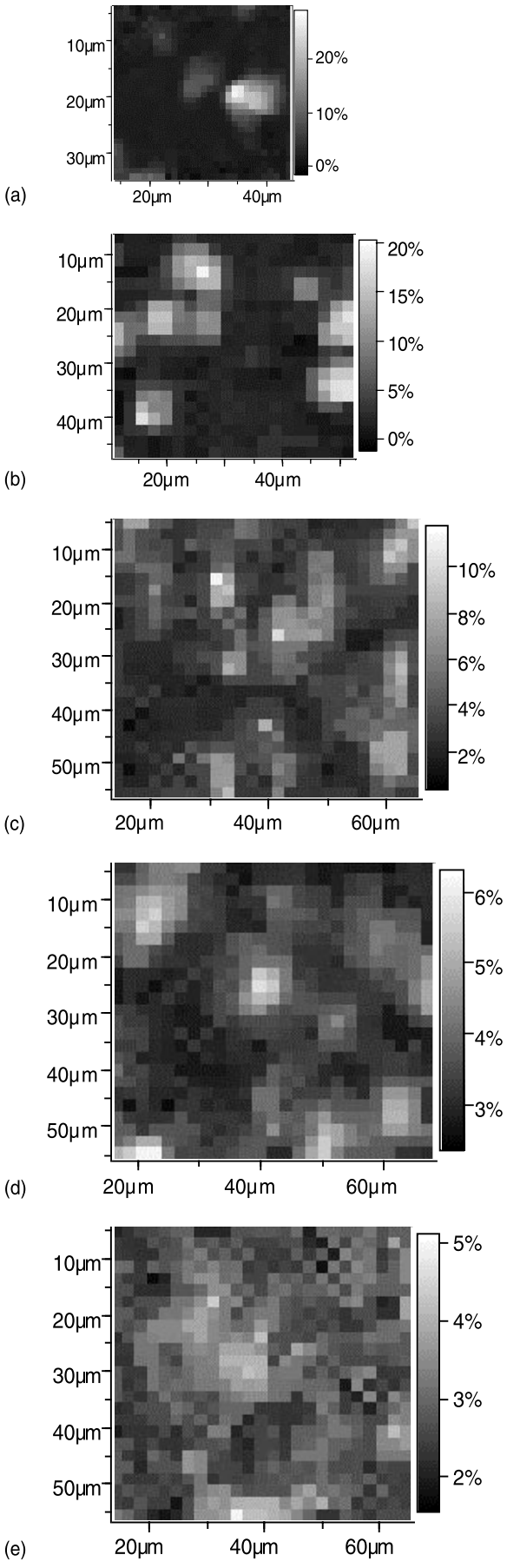

crystallized sample disappeared during holding at 150°C to give a homogeneous melt. In Ref. [23] we reported that homogeneous compositional images were obtained from quenched samples displaying a morphological phase structure when examined in the TEM. However, since the scale of the phase structure was close to the spatial resolution of the Raman technique there was some uncertainty regarding the interpretation of the images. In the present case the scale of the phase structure is much greater than the limit of spatial resolution and, consequently, we can be more certain that the polyethylene blend samples are compositionally homogeneous to within the error of compositional measurement (±1%). Fig. 4 shows a TEM micrograph of the isothermally crystallized and remelted (48 h at 150°C) 10% blend. The sample displays a biphasic morphology of the type commonly observed after quenching blends which are rich in branched polyethylene. There are regions containing only thinner crystals and separate, banded regions containing thicker crystals. The association of a biphasic morphology with a melt which has apparently remixed to uniform composition, raises further questions concerning the origin of the morphology. Before discussing the origin of the morphologies in more detail, further remixing experiments will be reported.

In order to study the remixing in greater detail a second phase stability experiment was performed. Compositional Raman images were recorded from isothermally crystallized 4% blends, after remelting and holding for a series of different times in the melt. The following holding times were used: 2 min, 20 min, 2 h and 5 h. Different samples were studied in each case so the images are not directly comparable, however, sufficiently large areas were studied for us to be sure that the images were representative of the whole sample. The Raman image of the initial material, before remelting, is reproduced in Fig. 5a from Ref. [23]. The Raman images of the remelted samples are shown in Fig. 5b–e. Each image in Fig. 5 has been generated using a spatial filtering procedure[2], which we believe to be useful for improving the quality of images of structures on a scale of five microns or more.

The Raman image recorded after 2 min at 150°C, see Fig. 5b, is similar to that recorded for the initial material. There are large compositional differences across the image, and the diameters of the DLPE rich phases are 5–10 μm. Although the maximum DLPE content is 9% lower in the

[2] The spatial filtering procedure removes noise spikes in the image in the following manner: the composition of each pixel is compared with those of its n neighbours. The composition of the central pixel is replaced by the median average of the $n + 1$ pixels. If the variation in composition in the $n + 1$ pixels is smooth, the median value is the same as the original composition of the central pixel; if not, the 'spike' is removed. In the present work the value of $n + 1$ was chosen to be 5. In images of structures on a scale significantly greater than the limit of spatial resolution of Raman imaging we believe it is a useful and legitimate precede for enhancing the data quality. In images of structures on the scale of the limit of the spatial resolution the procedure is not appropriate.

remelted sample than in the image of the initial sample, there are likely to be considerable variations in composition between DLPE rich phases. The similarity of the two images suggests that no significant diffusion had occurred during 2 min in the melt. The DLPE rich phases appear to spread out with longer times in the melt and the difference between the measured maximum and minimum DLPE contents decreases. The matrix phase increases in DLPE content and the DLPE rich domains decrease in DLPE content. Fig. 6 shows a plot of the maximum and minimum values of DLPE content in each of the spatially filtered Raman images shown in Fig. 5. After 5 h in the melt the compositional variations are very small and there has been little change in the detected compositional variation since the two-hour sample was taken. The filtered image of the five-hour sample does show a domain structure, but the compositional differences lie close to the error of ±1%. It would appear, therefore, that the ten-micron scale compositional phase structure in the isothermally crystallized sample remixes fully during approximately 5 h at 150°C.

The series of compositional profiles detected by Raman imaging as a function of time can be compared with theoretical profiles. The theoretical profiles are calculated using an estimated diffusion rate, D, for the DLPE and a solution of the diffusion equation:

$$\frac{\partial^2 C}{\partial x^2} + \frac{\partial^2 C}{\partial y^2} + \frac{\partial^2 C}{\partial z^2} = \frac{1}{D}\frac{\partial C}{\partial t} \tag{1}$$

where C is concentration; x, y and z are dimensions and t is time.

The diffusion rate is estimated by using the rate of self-diffusion of a linear polyethylene of molecular weight, M, given by the empirical equation of Klein and Briscoe:

$$D = \frac{14 \times 10^{-6}}{M^2} \tag{2}$$

A diffusion rate of 0.04 μm^2/min. is obtained when the M_w of the DLPE, 2×10^5, is equated with M.

An appropriate solution to Eq. (1) has been calculated previously for the general case of a diffusing substance, with diffusion rate, D, which is initially distributed uniformly through a sphere of radius, a, at concentration, C_0, [32]. The concentration at radius, r, and time, t, is given by:

$$C = \frac{1}{2}C_0\left\{\mathrm{erf}\left(\frac{a-r}{2\sqrt{(Dt)}}\right) + \mathrm{erf}\left(\frac{a+r}{2\sqrt{(Dt)}}\right)\right\}$$

$$-\frac{C_0}{r}\sqrt{\left(\frac{Dt}{\pi}\right)}\left[\exp\left\{\frac{-(a-r)^2}{4Dt}\right\} - \exp\left\{\frac{-(a+r)^2}{4Dt}\right\}\right] \tag{3}$$

The diffusion profiles generated using Eq. (3) and the following values of parameters: $a = 4$ μm, $D = 0.04$ μm^2/min, $C_0 = 30\%$ DLPE; are shown in Fig. 7. Remixing to a variation in composition within the uncertainty in composition of the Raman images, ±1%, is predicted to take approximately 5 h. The predicted remixing rate and the measured remixing rate are compared in Fig. 6, by plotting the maximum predicted composition alongside the experimental data. The agreement between the two sets of data is reasonable, considering the likely initial variation in maximum phase composition between each DLPE rich domain. Indeed, had C_0 been taken to be 20%, the maximum DLPE content observed experimentally after 2 min remixing, then the agreement between predicted and measured data would have been even closer. The agreement between theoretical and experimental remixing rates supports the argument that the DLPE rich domains remix with residence time at 150°C to give a homogeneous melt. It would appear that the morphological phase structures observed in some

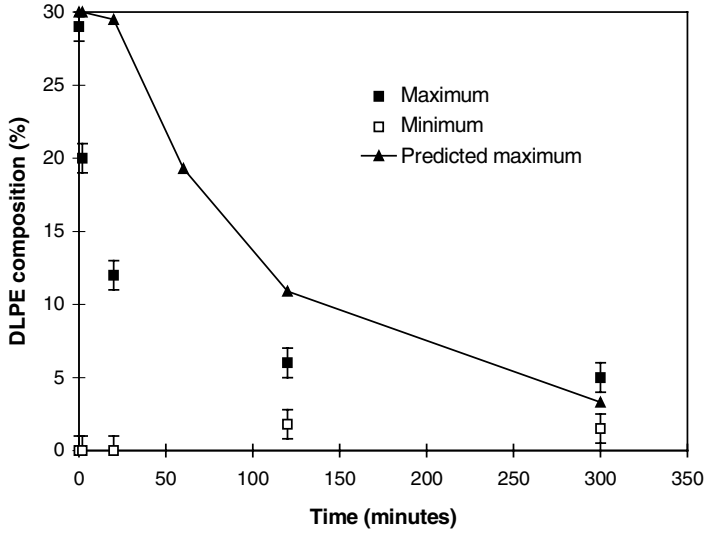

Fig. 6. Maximum and minimum DLPE compositions detected in the Raman images shown in Fig. 5 plotted as a function of time at 150°C. Theoretical maximum values derived from a diffusion calculation are plotted alongside the experimental data. Details of the calculation are given in the text.

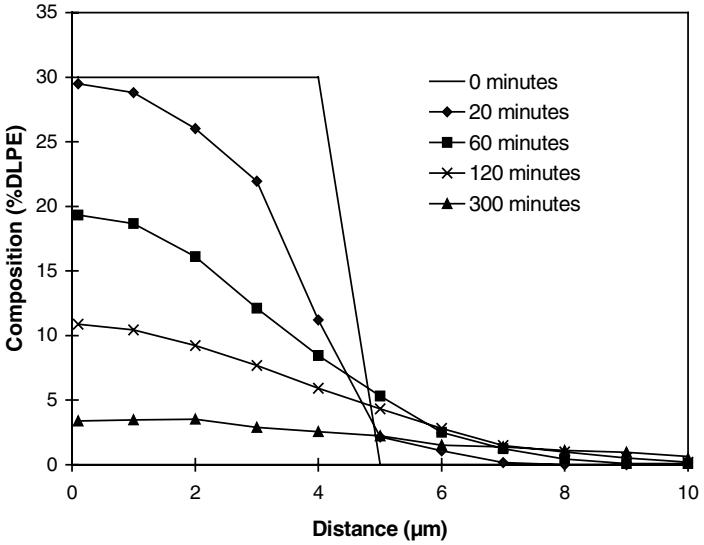

Fig. 7. Theoretical composition profiles plotted as a function of time. The profiles are derived from a diffusion calculation, details of which are given in the text.

quenched polyethylene blends cannot be associated with composition variations of greater than ±1%. Clearly, alternative explanations for the morphologies must be explored.

3.2. Crystallinity measurements

Raman imaging can be used to detect spatial variations in crystallinity through mapping the relative intensities of appropriate Raman bands. We have applied this technique to rapidly quenched blends displaying a morphological phase structure. Fig. 4, a TEM micrograph, shows the morphology of a 10% blend, quenched after holding at 150°C for 48 h following isothermal crystallization. Compositional and crystallinity Raman images were recorded from exactly the same area of a sample (the same sample, but not the same area as Fig. 4) and these are shown in Fig. 8. In Fig. 8a, the compositional image is shown for a 10% sample quenched after isothermal crystallization, followed by 48 h in the melt at 150°C. Our samples are blends, and so we are able to construct 'crystallinity images' for each component using the spectra recorded for each pixel. Examples of such spectra (for the extreme values) are shown in Fig. 8b–e. The resulting Raman images are presented in Fig. 8f (DLPE crystallinity) and Fig. 8g (BPE crystallinity). The scales used in the crystallinity images are simply the magnitudes of the appropriate Raman band ratios and are not crystallinities. In Fig. 8h and i we have modified the images in Fig. 8g and h, to bring out the complementary nature of the two crystallinities. The images have been smoothed, and, to make comparison simpler, in one of them (the DLPE image) the contrast has been inverted, so that dark regions now represent high crystallinity; if the crystallinities were exactly complementary Fig. 8h and i would look the same.

The Raman image in Fig. 8a displays little variation in composition and the spatial distribution of the small compositional differences appears to be random. Importantly, micron scale phases, each with a different composition, cannot be resolved. We have shown previously that, if the micron sized morphological phases seen in the electron micrograph, Fig. 4, were to be associated with compositional differences, these cannot be greater than 3% (absolute) [23]. In contrast to the compositional image, both of the crystallinity images exhibit a micron sized phase structure and the magnitudes of the differences in crystallinity are significant. The two Raman crystallinity images are approximately complementary and the phase structure is on a similar scale to that shown in the TEM images (e.g. Fig. 4).

A similar set of Raman images is shown in Fig. 9, this time for a single area of a sample with 4% DLPE. This sample was prepared in a different way from those previously discussed in this paper. The previous samples were crystallized isothermally, to produce large, well-separated areas of differing composition and these were subsequently held in the melt at 150°C. The sample of Fig. 9, however, was melted for 30 min at 190°C (quenching from this temperature gives a single morphology, see Fig. 1) and then held at 150°C for 30 min before being quenched; the corresponding TEM micrograph is shown in Fig. 10; it reveals a clear double morphology. The corresponding Raman images, Fig. 9, are all from the same sample area (they are from the sample shown in Fig. 10 but not from the area of Fig. 10). Again the compositional image shows little variation. Note that the range is rather less than in the sample shown in Fig. 5c — that 4% sample had been held at 150°C for 20 min, but it had been isothermally crystallized previously, to give large compositional differences, and these were still clearly evident after 20 min. Fig. 5e is also of interest here, that sample had been stored for 5 h at

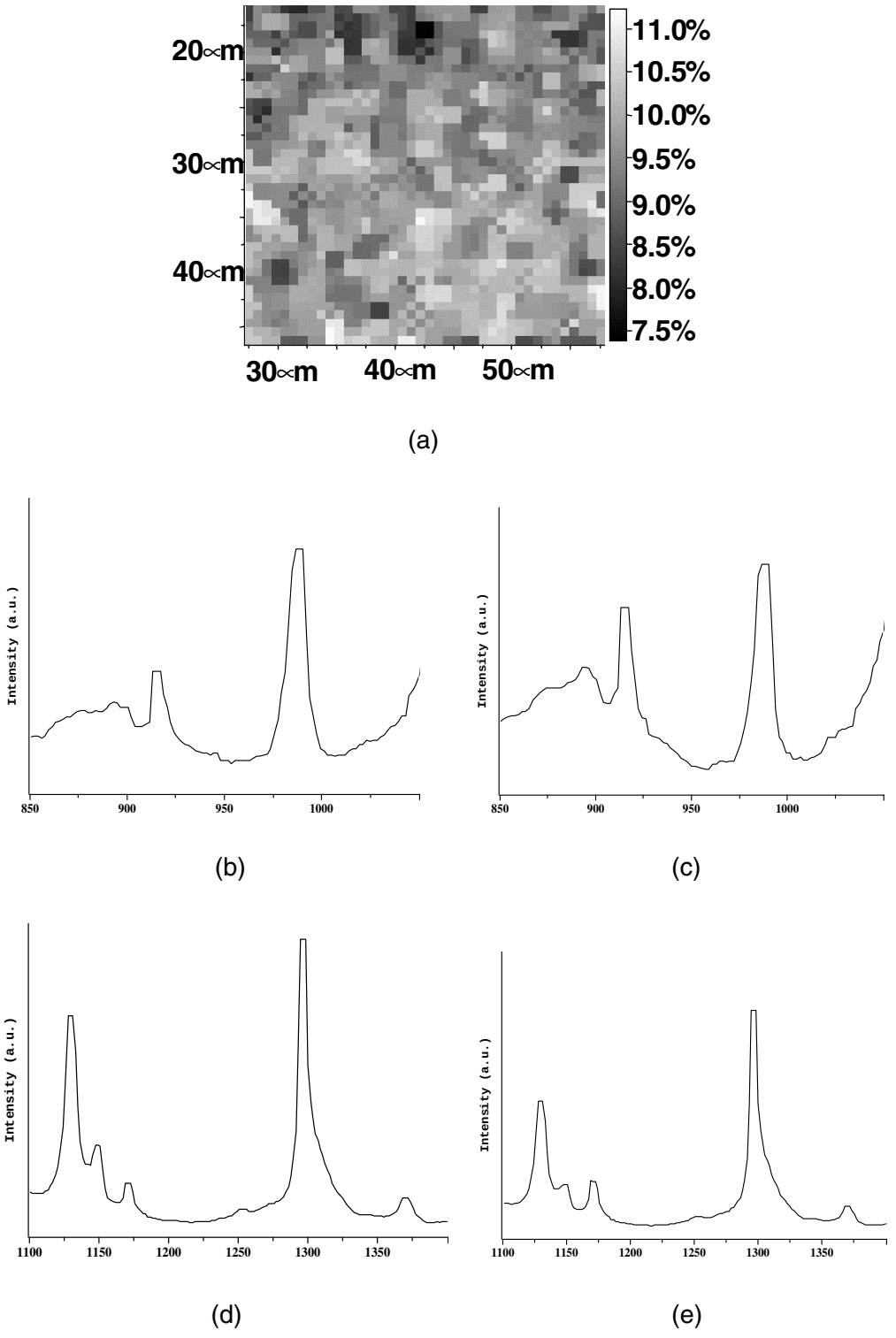

Fig. 8. Raman images and spectra of a 10% DLPE/BPE blend, isothermally crystallized (118°C), then held at 150°C for 48 h before quenching. N.B. all the Raman images are taken from the same sample area. (a) Compositional image based on the ratio of the integrated areas of the Raman bands at 2100 cm^{-1} (CD_2 stretching) and 2900 cm^{-1} (CH_2 stretching). The image is similar to the image in Fig. 3b, but is of a different area of sample and is reproduced here only to enable a direct comparison with the crystallinity images; (b)–(e) Parts of the Raman spectra of DLPE and of BPE, of high and low crystallinity, respectively; (f) DLPE crystallinity image based on the ratio of the integrated areas of the Raman bands at 986 and 914 cm^{-1}; (g) BPE crystallinity image based on the ratio of the integrated areas of the Raman bands at 1130 and 1295 cm^{-1}; (h) as (f), but now the image is smoothed and made negative; (i) as (g), but now the image is smoothed.

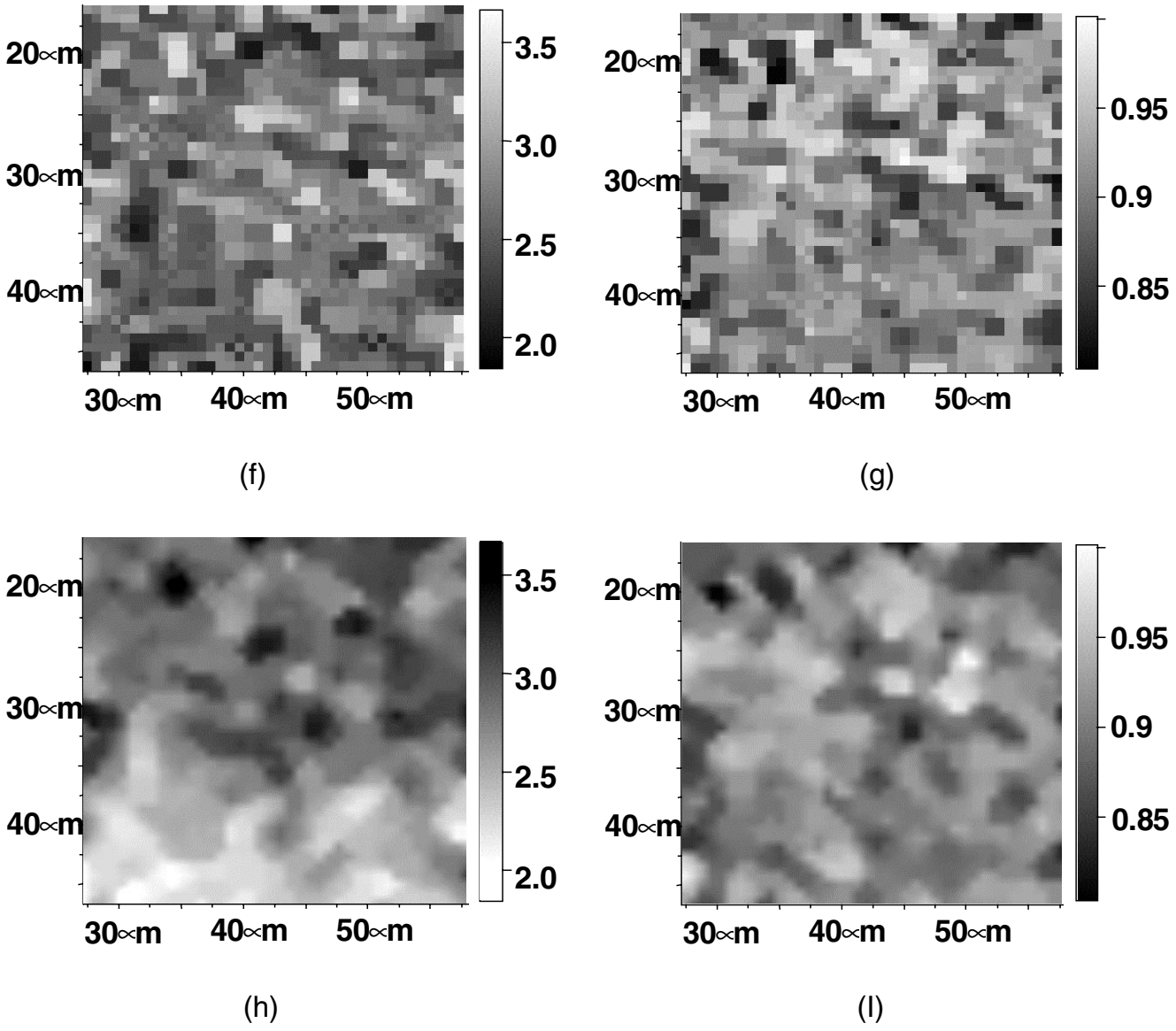

Fig. 8. (*continued*)

150°C following isothermal crystallization, and it shows a wider range of composition than the sample in Fig. 9a, which had never been crystallized isothermally. Although the compositional image (Fig. 9a) shows very little variation, the two crystallinity images show significant variations, and, as for the 10% sample in Fig. 8, the DLPE and BPE images are complementary.

The maximum pixel magnitude in the images for the DLPE crystallinity is about twice that of the minimum pixel magnitude for both the 4 and 10% samples. This suggests that the crystallinity of the DLPE, in the darker regions of Figs. 8f and 9f, may be as low as half that of the lighter regions.

Looking at the crystallinity maps for the BPE components, we see that the magnitudes of relative band intensity variations are smaller. The maximum pixel magnitude is 1.3 times greater than the minimum pixel magnitude, suggesting a difference of up to about 30% in the crystallinity of the BPE in the two regions.

Comparisons of Fig. 8f with g and of Fig. 9f with g (perhaps displayed more clearly in the smoothed images, Figs. 8h, i and 9h, i) show that the regions of high DLPE crystallinity correspond to the regions of low BPE crystallinity and vice versa in both sample types. Taken together, we believe the two crystallinity images represent convincing evidence for there being a correlation between morphological variations and crystallinity variations. We conclude that, while the composition is uniform through the sample, there is one kind of area where the branched polymer is more frequently incorporated in the crystals

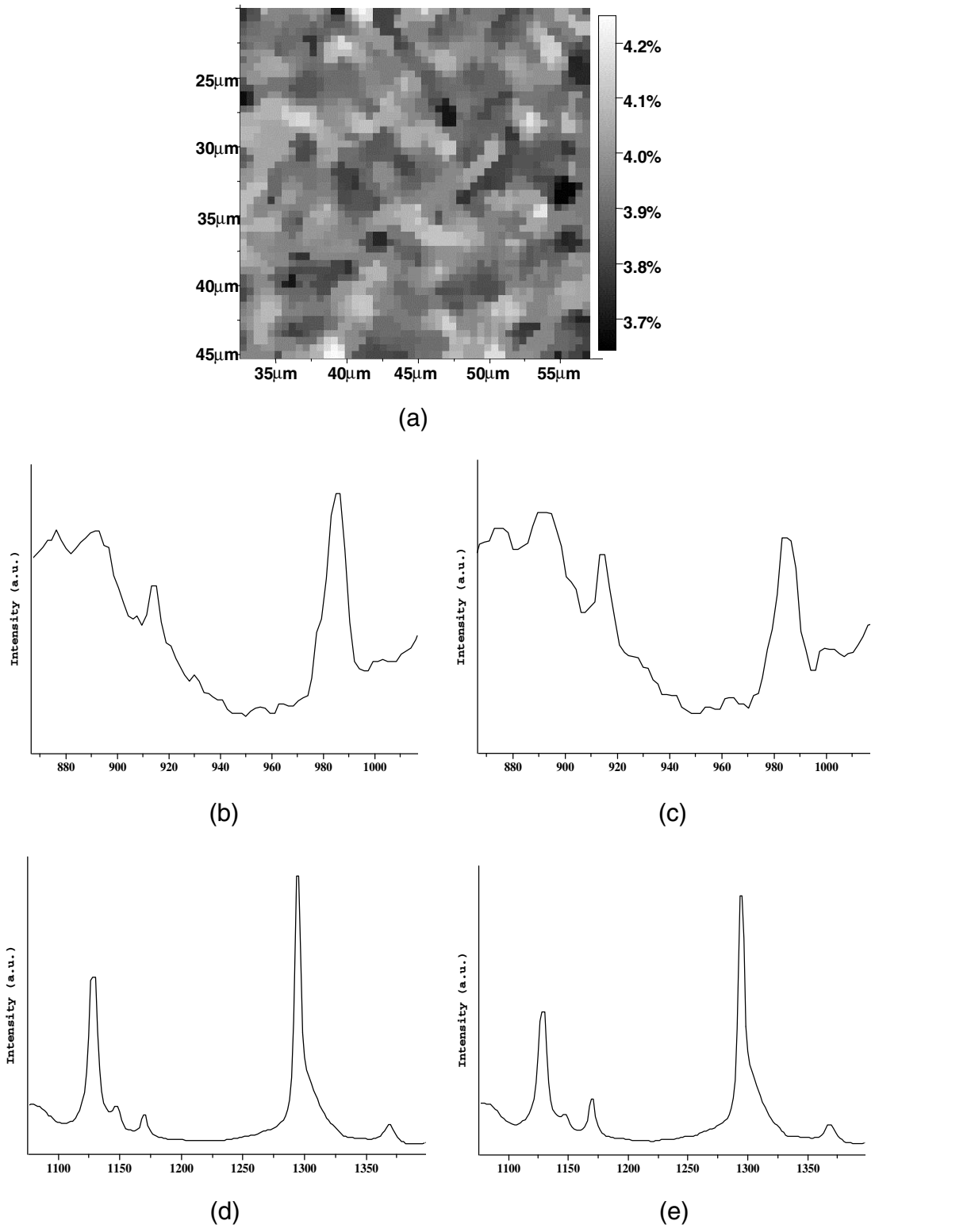

Fig. 9. Raman images and spectra of a 4% DLPE/BPE blend, rapidly quenched after melting at 190°C for 30 min, cooling to 150°C and holding for a further 30 min. N.B. all the images were taken from the same sample area. (a) compositional image based on the ratio of the integrated areas of the Raman bands at 2100 cm^{-1} (CD_2 stretching) and 2720 cm^{-1} (CH_2 stretching); (b)–(e) Parts of the Raman spectra of DLPE and of BPE, of high and low crystallinity, respectively; (f) DLPE crystallinity image based on the ratio of the integrated areas of the Raman bands at 986 and 914 cm^{-1}; (g) BPE crystallinity image based on the ratio of the integrated areas of the Raman bands at 1130 and 1295 cm^{-1}; (h) as (f), but now the image is smoothed and made negative; (i) as (g), but now the image is smoothed.

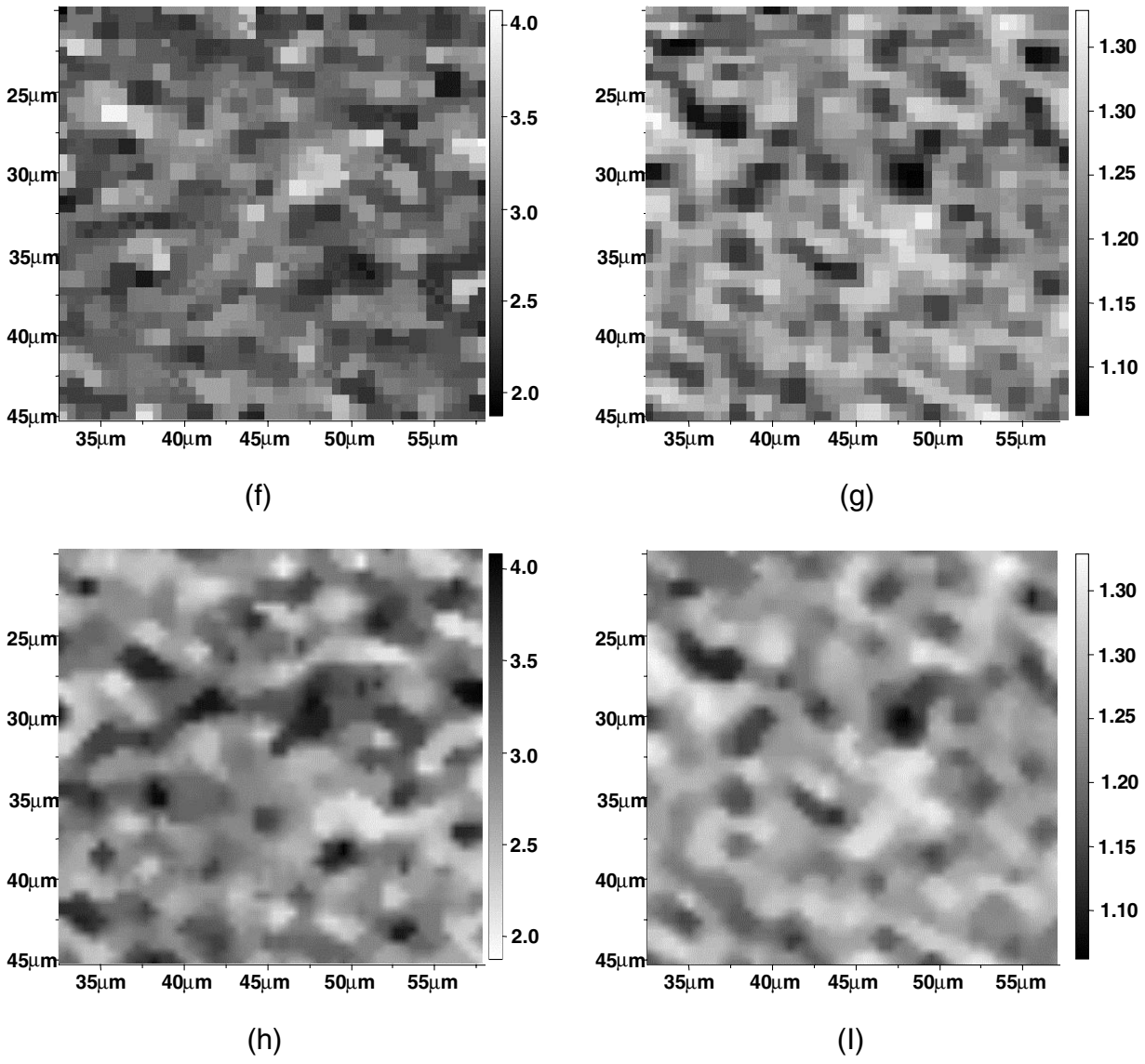

Fig. 9. (*continued*)

(leading to a higher value for the BPE crystallinity), and a second kind of area where the crystallinity of the LPE is higher. The size scales of these regions are directly comparable with the morphologically distinct regions seen in the TEM. We believe that the two morphologically distinct regions that we see in electron micrographs correspond to zones where the crystallinity of the branched polymer is particularly high and zones where it is significantly lower.

Note that the uniformity of composition, coupled with crystallinity difference is observed for two different types of quenched samples after storage in the melt in the 'biphasic morphology region'. Some samples experienced isothermal crystallization (to give large-scale composition differences) before storage in the melt in the 'biphasic morphology region' (Fig. 8); others were believed, on morphological evidence, to have a uniform composition before storage melt (Fig. 9).

Unfortunately, we are not able to perform TEM and Raman imaging over exactly the same area of sample and so we cannot ascertain whether there is spatial correspondence between the crystallinity and morphological phases, nor can we directly assess which crystallinity phase corresponds to which morphological phase. None-the-less, from the amounts of the two components observed, we believe that the regions in the micrographs consisting of smaller lamallae correspond to those with the higher BPE crystallinity, and that the regions of thicker crystals (arranged in banded structures) correspond to a higher LPE crystallinity.

3.3. 'Phase behaviour' of polyethylene blends

We reiterate here that, in all our previous studies, we have consistently found that the appearance of biphasic morphologies depends on: the branch content of the BPE; the actual

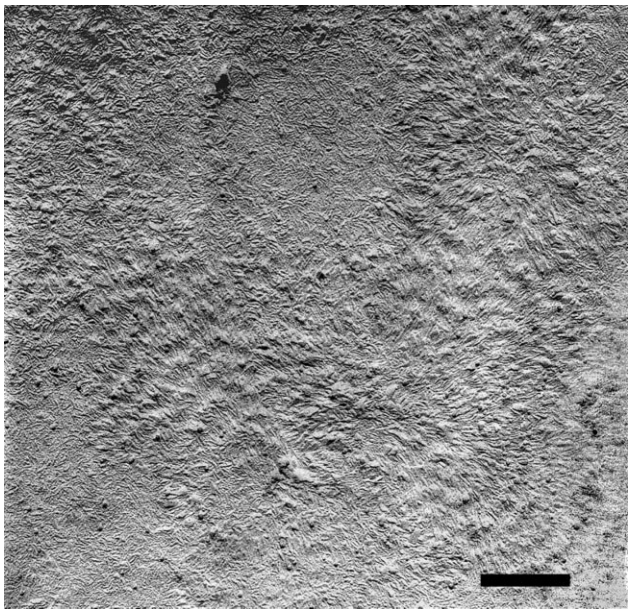

Fig. 10. Transmission electron micrograph of a replica of a 4% DLPE/BPE blend sample, this is the same sample, but not the same sample area, as that used for the Raman images seen in Fig. 9. There are micron-sized domains of thicker crystals arranged in a banded texture, one such is seen below centre. The scale bar represents 1 μm.

blend composition; the temperature at which the melt is held; and, importantly, the time for which a blend sample is held in the melt, with longer holding times generally leading to larger scale domain structures in the quenched samples. All this is strongly suggestive that the underlying cause is some form of phase separation occurring in the melt.

However, the Raman studies reported above show that the concentrations of the polymers within each morphological phase do not differ. Accordingly, any phase separation of the size scale observed in the TEM that may occur in the melt is not, as we have previously suggested, on the basis of branch content. In addition, SANS results, reported in detail elsewhere [20,15] and discussed above in Section 1, indicate that there is no widespread, small-scale phase separation in the melt on the basis of branch content. In contrast, the present Raman studies also show that there are clear and significant, differences in DLPE and BPE crystallinities in regions of the quenched blend, and that these are on the same spatial scale as the morphological differences observed in the electron micrographs. We therefore argue, it is at least possible, that there is some phase separation process occurring in the melt which, after quenching, leads to the formation of zones of relatively higher and lower, crystallinity of the components. There are several possible explanations, two of which we discuss below.

1. There may be phase separation by molecular weight, leading to some crystals being composed of higher molecular weight molecules taken from both DLPE and BPE. On the basis of the generality of the morphology maps [1], and of the apparent lack of sensitivity to molecular weight averages [4,5] and distributions [8,18], this seems unlikely.
2. There may be phase separation of nucleation sites. These nucleation sites might be composed of LPE of some degree of order, either static or more likely dynamic. If there are some well-separated, highly effective, nuclei in the melt then it is possible that upon quenching the crystals will start growing at these nucleation sites at comparatively high temperatures where only the more linear molecules are able to crystallize, leading to regions of high linear crystallinity. Then, when the temperature is low enough, nucleation may occur very rapidly at the separated, less-effective nucleation sites and the branched material may be caught up in the quickly growing crystals leading to regions where there is a relatively high crystallinity of the branched polymer. This model might also explain the limitation on the composition for the double morphology to occur. This model might also explain the limitation on the composition for the double morphology to occur. If the concentration of nucleation sites is too high, then the two separate domains might be too interfused to show up as separate domains in electron micrographs. In contrast, if the concentration of the LPE is very low, not enough nucleation sites will be present, leading to the formation of only a few domains of higher LPE crystallinity, unnoticeable in electron micrographs. This could explain the observation of morphology maps like that shown in Fig. 1.

4. Conclusions

The Raman data clearly show that in rapidly quenched blend samples where a biphasic morphology can be seen by electron microscopy, there are two distinct regions separated on a similar scale to the morphologically distinct regions seen in the electron microscope. The Raman data also clearly demonstrate that the distinguishing feature of these regions is not their relative branch content, but rather the degree of crystallinity of the two components. Accordingly, we conclude that the morphological differences that we have previously assigned to differences in branch content should, correctly, be attributed to differences in the crystallinity of both the branched and linear molecules.

It is clear from all previous evidence that the branch content of the BPE, the actual blend composition, the temperature at which the melt is held, and the time for which a blend sample is held in the melt, all affect the morphologies observed on quenching. The simplest argument is that there is some sort of phase separation — it could be on the basis of molecular weight, on the basis of nucleation or for some other, as yet unidentified, reason. The

present Raman results, however, indicate that any phase separation is not on the basis of branch content.

Acknowledgements

R.L. Morgan, M.J. Hill, P.J. Barham wish to thank BP Chemicals, DSM and Solvay for a grant to support this work.

References

[1] Crist B, Hill MJ. J Polym Sci, Part B: Polym Phys 1997;35:2329.
[2] Barham PJ, Hill MJ, Keller A, Rosney CCA. J Mater Sci Lett 1988;7:1271.
[3] Hill MJ, Barham PJ, Keller A, Rosney CCA. Polymer 1991;32:1384.
[4] Hill MJ, Barham PJ, Keller A. Polymer 1992;33:2530.
[5] Hill MJ. Polymer 1994;35:1991.
[6] Hill MJ, Barham PJ. Polymer 1992;33:4099.
[7] Hill MJ, Barham PJ. Polymer 1992;33:4891.
[8] Hill MJ, Barham PJ, Van Ruiten J. Polymer 1994;34:2975.
[9] Barham PJ, Hill MJ, Goldbeck Wood G, Van Ruiten J. J Polym 1994;34:2981.
[10] Thomas D, Williamson J, Hill MJ, Barham PJ. Polymer 1993;34:4919.
[11] Hill MJ, Barham PJ. Polymer 1994;35:1802.
[12] Hill MJ, Organ SJ, Barham PJ. Thermochim Acta 1994;238:17.
[13] Puig CC, Odell JA, Hill MJ, Barham PJ, Folkes MJ. Polymer 1994;35:245 211.
[14] Hill MJ, Barham PJ. Polymer 1995;36:3369.
[15] Schipp C, Hill MJ, Barham PJ, Cloke V, Higgins JS, Olazabal L. Polymer 1996;37:2291.
[16] Morgan RL, Hill MJ, Barham PJ, Frye CJ. Polymer 1997;38:1903.
[17] Hill MJ, Morgan RL, Barham PJ. Polymer 1997;38:3003.
[18] Hill MJ, Barham PJ. Polymer 1997;38:5595.
[19] Hill MJ, Puig CC. J Appl Polym Sci 1997;65:1921.
[20] Alamo RG, Londono JD, Mandelkern L, Stehling FC, Wignall GD. Macromolecules 1994;27:411.
[21] Londono JD, Narten AH, Wignall GD, Honnell KG, Hsieh ET, Johnson TW, Bates FS. Macromolecules 1996;29:5332.
[22] Morgan RL, Hill MJ, Barham PJ. Polymer 1999;40:337.
[23] Morgan RL, Hill MJ, Barham PJ, Markwort L, Kip BJ, Van Ruiten J, Van der Pol A. J Macromol Sci — Phys 1999;B38:419.
[24] Kip BJ, Meier RJ. Appl Spectrosc 1990;44:707.
[25] Markwort L, Kip BJ, DaSilva E, Roussel B. Appl Spectrosc 1995;49:1411.
[26] Strobl GR, Hagedorn W. J Polym Sci: Polym Phys Ed 1978;16:1181.
[27] Naylor CC, Meier RJ, Kip BJ, Williams KPJ, Maison SM, Conroy N, Gerrard DL. Macromolecules 1995;28:2969.
[28] Snyder RG. J Mol Spectrosc 1970;36:222.
[29] Patrick M, Bennett V, Hill MJ. Polymer 1994;37:5335.
[30] Bassett DC, Hodge AM. Proc R Soc A 1978;359:121.
[31] Olley R, Hodge AM, Bassett DC. J Polym Sci, Polym Phys 1979;17:627.
[32] Crank J. The mathematics of diffusion. 2nd ed. Oxford: Clarendon Press, 1979.